Electronic Supplementary Information (ESI)

Title

Smart electrically responsive hybrid ion-selective membranes for selective gated transport of ionic species

Authors

Francois-Marie Allioux[1], Sébastien Balme[2], Ludovic F. Dumée[1*]

Affiliations

[1] Deakin University, Geelong, Institute for Frontier Materials, Victoria, 3216, Australia

[2] Institut Européen des Membranes, Montpellier, France

Corresponding author[*] Ludovic.dumee@deakin.edu.au

Electronic Supplementary Information (ESI)

1. Experimental section

1.1 Materials and Chemicals

Aqueous salt solutions were prepared using deionized (DI) water. Sodium chloride (NaCl, AR grade, > 99.7% purity, $M_w = 58.44$ g.mol^{-1}), sodium sulphate anhydrous (Na_2SO_4, analytical grade, > 99% purity, $M_w = 142.04$ g.mol^{-1}), sodium hydroxide (NaOH, AR grade, > 99% purity, $M_w = 40.01$ g.mol^{-1}) and hydrochloric acid (HCl, AR grade, 32% w/w) were purchased from ChemSupply, SA, Australia.

1.2 Preparation of the hybrid IEMs

The electrically-responsive hIEMs were prepared as a two-phases composite material comprised of an inorganic and electrically conductive reinforcing fabric embedded into an ion-selective polymeric paste.[1] Briefly, the hIEMs were prepared using a pore filling method previously applied to polymeric reinforced IEMs.[2, 3] A porous stainless steel woven wire cloth obtained from FuelCellStore (TX, USA), 70 × 70 in mesh size (Fig1. a), was used as an inorganic and electrically conductive reinforcement for the fabrication of the hIEMs. The ion-selective phase of the hIEMs was composed of a heterogeneous anion or cation-exchange polymeric paste made of a fine powder of commercial resin beads dispersed into a poly(vinyl chloride) (PVC) polymer binder.[1] Amberlyst® 15 strong cation-exchange resin was supplied by Sigma-Aldrich, Castle

Hill, NSW. Amberlyst® 15 is a nanoporous styrene-divinylbenzene matrix with sulfonic acid (-SO_3^-) as fixed functional groups (Table S1) [4]. Amberjet® 4200 chloride form, anion-exchange beads (Cl^- form) was also purchased from Sigma-Aldrich. Amberjet® is a strong base anion-exchange resin with trimethyl ammonium groups (-$N^+(CH_3)_3$) as fixed functional groups within a styrene-divinylbenzene copolymer matrix [4]. The full fabrication details and extended characterization of the hybrid membranes can be found in our precedent publications.[1, 5, 6]

1.3 Hybrid material characterization

The characterization of the chemical functional groups present at the surface of the hybrid materials was performed using Attenuated Total Reflectance Fourier Transform Infrared (ATR-FTIR) techniques. Spectra were acquired on a Bruker Vetex-70 FTIR spectrometer and recorded in the range of 600 - 4000 cm^{-1} at a resolution of 4 cm^{-1}. A total of 64 spectra were averaged for each measurement.

The morphologies of the stainless-steel reinforcement and hIEMs were studied by SEM on a JEOL JSM 7800F model. SEM imaging were performed at 10 keV and 10 mm working distance. The hybrid SEM samples were gold coated (model SCD 050 sputter coater, Bal-Tec) prior to imaging with a 5-nm thick layer of gold.

1.4 Capacitive ED set-up

The capacitive ED tests were performed in a laboratory scale ED cell made of poly(methyl methacrylate) (PMMA) previously designed to investigate the desalination performance of the novel hIEMs in conventional ED with model salt solutions. The membrane stack was composed of a single pair of hybrid cation and anion-exchange membranes (hCEM and hAEM, respectively) forming the diluate compartment and an additional hAEM placed next to the electrode to separate the concentrate from the electrode stream as illustrated in Fig. 1b. The diluate and concentrate compartments were formed using PMMA spacers with serpentine hydraulic pathways, which present an effective transfer area of 4.60 cm^2. The specific width and depth of the hydraulic channels were 3.4 and 2 mm, respectively.

The fluid flow velocity across the spacers was set at 4.3 $cm.min^{-1}$, which represented a flow rate of 18 $mL.min^{-1}$. The concentrate and diluate were fed by solutions of the same ionic strength and composition (1 L of solution per compartments in volume) to prevent any excessive concentration gradient and osmotic diffusion across the IEMs. The contribution of the pure diffusion regime was therefore considered negligible on the ionic mass transport at the start of the experiments. Furthermore, cross-flow rates were applied across the compartments to reduce concentration gradients. The electrode compartments were fed with a solution of Na_2SO_4 in DI water (4 wt%). The feed, concentrate and electrode streams were recirculated across the ED stack with a 4-head peristaltic pump (John Morris, Scientific, USA).

A DC power supply (BK Precision, 9124, LabVIEW software) was used to control and data-log the experimental current and voltage applied across the two gold electrode plates (40 x 40 mm^2) forming the ED module. A small portion of the stainless steel (SS) substrates composing the hybrid materials was exposed and wired to an external and second DC power supply (similar BK Precision, 9124 model) to polarize the hIEMs and tune the electrical field across the diluate compartment as represented in Fig. 1c.

The conductivity (χ), temperature (T) and pH of the feed and product solutions were recorded using a conductivity meter (CondTPS, WP-81) in automatic temperature compensation mode and data-logged with the software Termite (CompuPhase, USA). In addition, the gas produced at the electrodes or across the compartments during ED process was qualitatively analyzed using a handheld gas sensor (MultiRAE lite, RAE Systems, US).

1.5 Ionic fluxes calculation

Salt fluxes and permeations were calculated from the salt concentration variation for set time periods ($\frac{dC_{Salt}}{dt}$) across the feed and product compartments [7]. The experiments were performed at room temperature and tests were carried out in recycled mode configuration. The ionic fluxes through IEMs were defined from Equation S1.

$$J_{Salt} = \frac{V * \frac{dC_{Salt}}{dt}}{A} \qquad \text{Equation S1}$$

Where V is the volume of solution (L), A the membrane active surface area (cm^2) and $\frac{dC_{Salt}}{dt}$ is in mol.L^{-1}.s^{-1}.

1.6 Ion-exchange capacity (IEC)

The IECs of the hIEMs were obtained by titration method. Dry hIEM samples were prepared and weighed (m_{dry}). hCEMs in acid form and hAEMs in alkaline form were equilibrated, respectively, in a 1 mol.L^{-1} NaCl solution and a 0.05 mol.L^{-1} hydrochloric acid (HCl) solution for 48 h. H^+ ions in solution were then titrated with a NaOH solution and phenolphthalein indicator. Measurements were performed on 3 different samples. IECs were calculated following the equation [8-10]:

$$IEC\left(mmol.g^{-1}\right)=\left(\frac{n1,\ HCl\ -\ n2,HCl}{m_{dry}}\right) \qquad \text{Equation S2}$$

Where m_{dry} is the mass of dried membrane sample and n1,HCl – n2,HCl

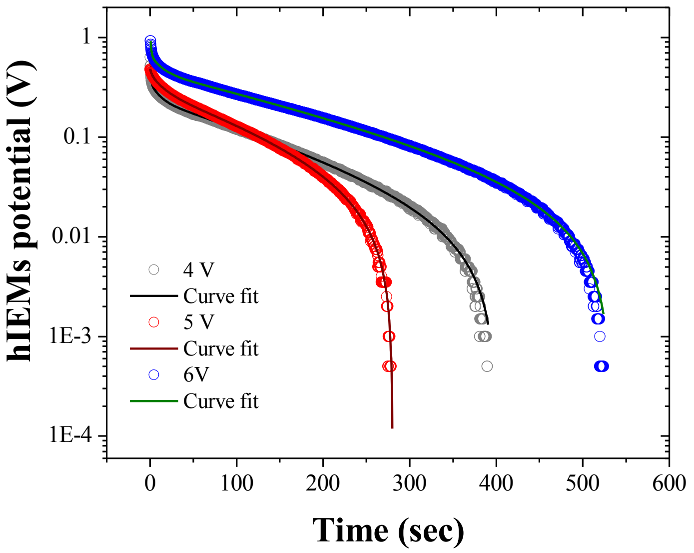

Fig. S1. Non-linear fittings of the potential (V) discharge behavior across the hIEMs. Fittings were performed using a three integrators law corresponding to a network of RC circuit arranged in parallel.**[11]**

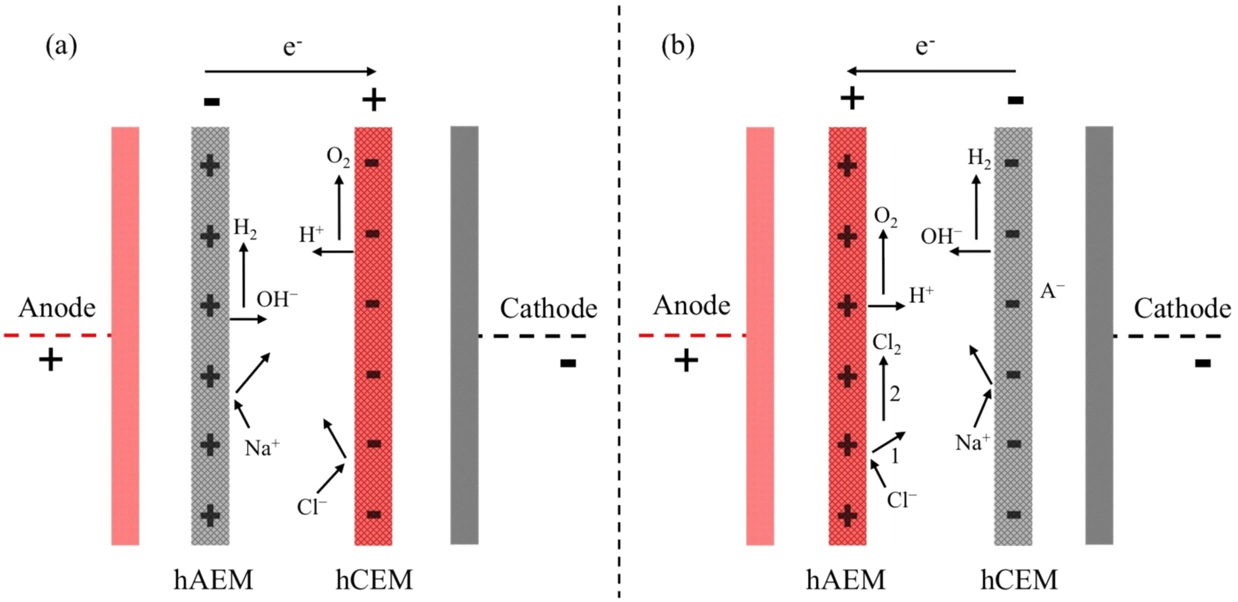

Fig. S2. Schematic representation of the reactions occurring at the surface of the hybrid IEMs when (a): a negative and (b): a positive potential is applied across the pair of hybrid IEMs in the ED cell.

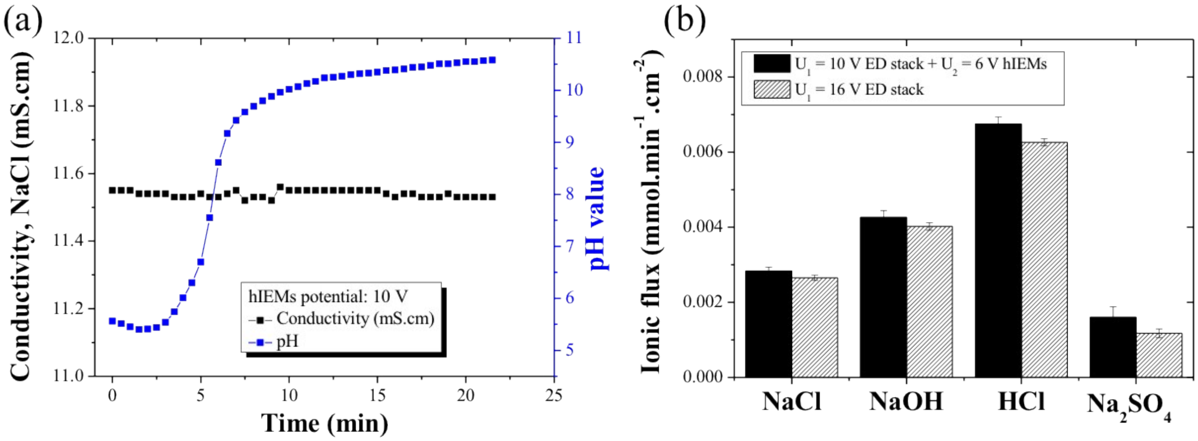

Fig. S3. (a): Change of conductivity and pH as a function of the ED time for an applied potential of 10 V across the pair of hybrid IEMs only. (b): Ionic fluxes of the studied salts across the diluate compartment. Salt initial concentrations were set at 0.01 M

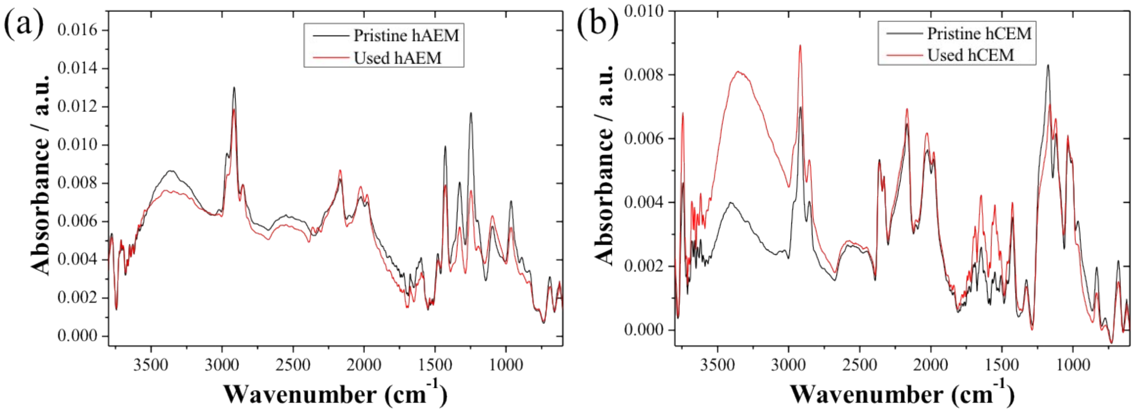

Fig. S4. FTIR spectra of the (a): hAEMs and (b): hCEMs before and after capacitive ED experiments.

Table S1. Properties of the hybrid IEMs

Properties	**hAEM**	**hCEM**
Membrane thickness (μm)	205 ± 9	200 ± 3
Material resistivity ($\Omega.cm^2$)	8.15	2.92
Water uptake (wt%)	22 ± 3	26.2 ± 2.1
IEC (meq/g)[1] [1]per grams of hybrid material	Pristine: 0.92 ± 0.1 Used: 1.05 ± 0.12	Pristine: 1.11 ± 0.11 Used: 0.91 ± 0.09
Ion-exchange functional groups	$-N^+(CH_3)_3$	$-SO_3^-$

1. Allioux, F.-M., et al., Investigation of hybrid ion-exchange membranes reinforced with non-woven metal meshes for electro-dialysis applications. Separation and Purification Technology, 2015. 147: p. 353-363.
2. Yamaguchi, T., F. Miyata, and S.-i. Nakao, Pore-filling type polymer electrolyte membranes for a direct methanol fuel cell. Journal of Membrane Science, 2003. 214(2): p. 283-292.
3. Seo, S.-J., et al., Electrochemical properties of pore-filled anion exchange membranes and their ionic transport phenomena for vanadium redox flow battery applications. Journal of Membrane Science, 2013. 428(0): p. 17-23.
4. Sigma-Aldrich. Amberlite and Amberlyst Resins - Technical Information Bulletin. [cited 2017 12/03/2017]; Available from: http://www.sigmaaldrich.com/chemistry/chemical-synthesis/learning-center/technical-bulletins/al-142/amberlite-amberlyst.html.
5. Dumée, L.F., et al., Qualitative spectroscopic characterization of the matrix–silane coupling agent interface across metal fibre reinforced ion exchange resin composite membranes. Vibrational Spectroscopy, 2014. 75: p. 203-212.
6. Allioux, F.-M., et al., Insights into Free Volume Variations across Ion-Exchange Membranes upon Mixed Solvents Uptake by Small and Ultrasmall Angle Neutron Scattering. ACS Applied Materials & Interfaces, 2017. 9(10): p. 8704-8713.
7. Balster, J., et al., Preparation and characterisation of monovalent ion selective cation exchange membranes based on sulphonated poly(ether ether ketone). Journal of Membrane Science, 2005. 263(1–2): p. 137-145.
8. Hu, J., et al., Plasma-grafted alkaline anion-exchange membranes based on polyvinyl chloride for potential application in direct alcohol fuel cell. Journal of Power Sources, 2011. 196(10): p. 4483-4490.
9. Lin, X., et al., A convenient, efficient and green route for preparing anion exchange membranes for potential application in alkaline fuel cells. Journal of Membrane Science, 2013. 425–426(0): p. 190-199.
10. Hosseini, S.M., et al., Fabrication of (polyvinyl chloride/cellulose acetate) electrodialysis heterogeneous cation exchange membrane: Characterization and performance in desalination process. Desalination, 2012. 306(0): p. 51-59.
11. Sierociuk, D., et al., Diffusion process modeling by using fractional-order models. Applied Mathematics and Computation, 2015. 257: p. 2-11.